Protein Structure

International Edition: DOI: 10.1002/anie.201504772
German Edition: DOI: 10.1002/ange.201504772

Structural Insights into the Incorporation of the Mo Cofactor into Sulfite Oxidase from Site-Directed Spin Labeling

*Aaron Hahn, Christopher Engelhard, Stefan Reschke, Christian Teutloff, Robert Bittl, Silke Leimkühler, and Thomas Risse**

Abstract: *Mononuclear molybdoenzymes catalyze a broad range of redox reactions and are highly conserved in all kingdoms of life. This study addresses the question of how the Mo cofactor (Moco) is incorporated into the apo form of human sulfite oxidase (hSO) by using site-directed spin labeling to determine intramolecular distances in the nanometer range. Comparative measurements of the holo and apo forms of hSO enabled the localization of the corresponding structural changes, which are localized to a short loop (residues 263–273) of the Moco-containing domain. A flap-like movement of the loop provides access to the Moco binding-pocket in the apo form of the protein and explains the earlier studies on the in vitro reconstitution of apo-hSO with Moco. Remarkably, the loop motif can be found in a variety of structurally similar molybdoenzymes among various organisms, thus suggesting a common mechanism of Moco incorporation.*

Molybdoenzymes play essential roles in many aspects of cell metabolism.[1] These molybdoenzymes are broadly conserved throughout evolution and share the so-called molybdenum cofactor (Moco). Human SO (hSO), which is localized to the intermembrane space of mitochondria, catalyzes the oxidation of sulfite to sulfate, the final step in the oxidative degradation of sulfur-containing amino acids, at its redox-active molybdenum cofactor. Sulfite, as a strong nucleophile, is able to cause severe damage to a multitude of cellular components including membrane components and sulfolipids.[1a] In the absence of SO, sulfite accumulates in the body and especially causes severe damage to the brain. The corresponding diseases, isolated sulfite oxidase deficiency[2] or Moco deficiency,[3] are characterized by rapidly progressing neurodegeneration[4] and death in early childhood.

In the past, molybdoenzymes were intensively studied to understand their enzymology, including their biosynthesis[5] and cellular distribution,[6] and the redox chemistry of the Moco.[7] However, elementary questions such as the molecular basis of the insertion mechanism of Moco into hSO remained open. Since hSO is localized to the intermembrane space of mitochondria, the mechanism of hSO translocation, assembly, and cofactor insertion is a complex, multistep maturation process, which has been proposed to be highly coordinated.[8] Owing to its instability, it is considered to be unlikely that Moco exists in a free protein-unbound form in the cell. However, Moco-binding chaperones for enzymes of the sulfite oxidase family have not been identified so far. Thus, several unexplored hypotheses exist for the insertion of Moco into hSO.[1a,9] Biochemical studies of SO and other molybdoenzymes suggest Moco to be the last cofactor inserted into the already assembled apoenzyme,[10] an observation that allows the structural details of the insertion step to be addressed by comparing the apo and the holo forms of the protein.

This study aims at elucidating the structural basis of the mechanism of Moco insertion into hSO by using site-directed spin labeling (SDSL). Human SO is a homodimer with a molecular mass of about 110 kDa and each monomer of the full-length protein consists of three domains referred to as the Moco, the heme-containing, and the dimerization domain. The structure of hSO has not been determined yet, however, a crystal structure was determined for the highly homologous chicken liver SO (cSO;[11] PDB ID: 1SOX, 67% identical residues).[12] Based on the structure of cSO, suitable labeling sites to probe structural changes within the Moco domain were selected and distance distributions between pairs of site-specifically introduced spin labels in the respective holo- and apoprotein samples were determined by using pulsed electron–electron double resonance spectroscopy (PELDOR or DEER) to search for structural changes related to the presence or absence of Moco.[13] The results reveal a highly localized change involving a short loop (residues 263–273 in hSO) in the Moco domain. This loop provides access to the Moco binding pocket from the outer surface in the apo form, while it blocks access in the holo form. The conservation of the loop structure as well as its binding motif for the Moco in a variety of structurally related molybdoenzymes (see Figure S12 in the Supporting Information) points to a conserved Moco insertion mechanism.

SDSL is typically based on the labeling of cysteine residues, which requires a construct without Cys to avoid interference with labeling at native cysteine residues. The cysteine-free construct used within this study lacks the N-terminal heme domain of hSO and is referred to as hSOMD (hSO Moco domain) throughout this study. It has previously

[*] Dr. A. Hahn, Prof. Dr. T. Risse
Institut für Chemie und Biochemie, Freie Universität Berlin
Takustr. 3, 14195 Berlin (Germany)
E-mail: risse@chemie.fu-berlin.de
C. Engelhard, Dr. C. Teutloff, Prof. Dr. R. Bittl
Fachbereich Physik, Freie Universität Berlin
Arnimallee 14, 14195 Berlin (Germany)
Dr. S. Reschke, Prof. Dr. S. Leimkühler
Institut für Biochemie und Biologie, Universität Potsdam
Karl-Liebknecht-Str. 24-25, 14476 Golm (Germany)
Dr. C. Teutloff, Prof. Dr. R. Bittl, Prof. Dr. T. Risse
Berlin Joint EPR Laboratory Freie Universität Berlin (Germany)

Supporting information for this article is available on the WWW under http://dx.doi.org/10.1002/anie.201504772.

been shown that the activity of hSOMD is retained after exchange of the four nonessential cysteine residues.[14] Additionally, 70–90% of wild type sulfite oxidation activity was obtained for all hSOMD variants containing the site-specifically introduced cysteine residues used in this study (at positions 195, 235, 302, 217, 267, 341, and 353) as long as the essential cysteine residue at position 207 was retained. Mutation of C207 to serine results in an inactive enzyme[15] owing to a loss of the cysteine-sulfur–molybdenum bond. Despite the lack of catalytic activity, all holo-form hSOMD variants lacking the essential residue C207 exhibited a molybdenum loading of about 80%, which corresponds to the molybdenum incorporation level of the wild-type protein as checked by inductively coupled plasma optical emission spectrometry (ICP-OES).

To verify the structural comparability of the cysteine-free hSOMD construct with the full-length wild-type protein (hSO), three sites located on different secondary structure elements, namely N195 (α-helix)[*], R235 (β-sheet), and R302 (loop) located around the Moco binding pocket were selected based on the cSO crystal structure (Figure 1). To investigate

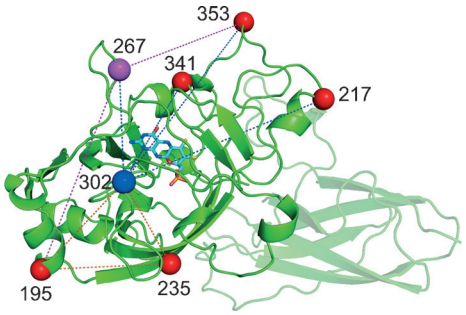

Figure 1. Residues selected for site-directed spin labeling (structure of cSO; PDB ID: 1SOX). Numbering corresponds to the respective positions in hSO. See the Supporting Information for sequence alignment.

the full-length hSO by SDSL, pairs of the non-natural amino acid *p*-acetylphenylalanine, namely N195/R235pAcPhe, N195/R302pAcPhe, and R235/R302pAcPhe, were introduced into the wild-type enzyme. These variants were labeled by using specific catalytic ketoxime coupling chemistry.[16] The distance distributions obtained for hSO were compared to theoretical expectations based on the cSO crystal structure using the PyMOL script "MtsslWizard",[17] which calculates the conformational space of different spin labels considering a simple van-der-Waals model. For all measurements, the resulting distance distributions as determined by using the software tool "DeerAnalysis 2013"[18] agreed well with expectations based on the crystal structure of cSO (Figure S2), a result that also holds for hSOMD variants containing the corresponding MTSSL-labeled cysteine pairs only. It should be noted that the distance distribution reveals contributions from spin–spin interactions within one (intra) and between the two (inter) monomer units of the homodimer. The simulations allow discrimination between them, and theoretical intramonomer distances are colored in blue while the inter-monomer distances are shown in green. The intermonomer distances are usually too large to be probed by the DEER experiments, therefore the discussion of the distance distribution is restricted to the intramonomer distances. Hence, hSOMD lacking the essential cysteine residue 207 and the full-length protein are structurally indistinguishable from cSO in the examined region. The cysteine-free hSOMD construct can be used as a reference for the apoprotein. It should be noted that ketoxime coupling of spin labels to apoprotein variants containing unnatural amino acids was not possible because of insufficient stability of the apoprotein under the reaction conditions.

The measurements for the apo forms of the hSOMD variants N195/R235C, N195/R302C, and R235/R302C revealed no changes, as expected based on the crystal structure of cSO (Figure S3, the distance distributions for all cysteine variants were calculated using both MtsslWizard as well as the Matlab toolbox "MMM2013.2" and they gave very similar results), hence, it is inferred that this region of the protein remains unperturbed in absence of the cofactor.

As a next step, the remaining secondary structure elements of the Moco domain of hSOMD were examined by using a variety of MTSSL-labeled cysteine pairs containing residue 302, shown to be fixed, with sites 217, 267, 341, and 353, as well as two additional pairs of residue 267 with residues 195 and 353 (Figure 1), which exhibit predicted intramonomer distances compatible with DEER experiments (15–60 Å[13]). For each pair, distance distributions were measured for the holo- and apoproteins. For the traces with modulation depths approaching 0.5 (e.g., the holo form of variant 195–267C; Figure S5) multiple spin interactions within the homodimer have to be considered. These may lead to artificial contributions ("ghost peaks") in the distance distribution. However, data analysis using the "power-scaling" approach[19] implemented in "DeerAnalysis 2013" gave no indication of "ghost-peaks". The measurements on pairs 302–217, 302–341, and 302–353 showed no significant differences between the holo and apoprotein samples as exemplified for the latter pair in Figure 2A (for DEER traces, see Figure S4). Based on these results, it can be concluded that the structure of the protein as probed by these residues is unchanged after insertion of the Moco. A different scenario is found for pairs containing residue 267. Comparing, for example, the distance distributions of the apo- and holoproteins for the pair 195–267 shown in Figure 2B, a new peak at smaller distances together with some weight at distances between 30 and 50 Å is observed for the apo form of the protein. The contribution at small distances is readily seen in the time traces (Figure S5), which show a considerably faster initial decay of the DEER trace for the apo form, corresponding to shorter distances. While the interspin distance between 195–267 is reduced in the apo form, increased distances are observed for 267–302 (Figure 2C). Together with the observation that the distance distribution is virtually unchanged for all other pairs investigated, it is concluded that

[*] The numbering Scheme refers to hSO. Information on the sequence alignment as compared to cSO and its crystal structure may be found in the Supporting Information.

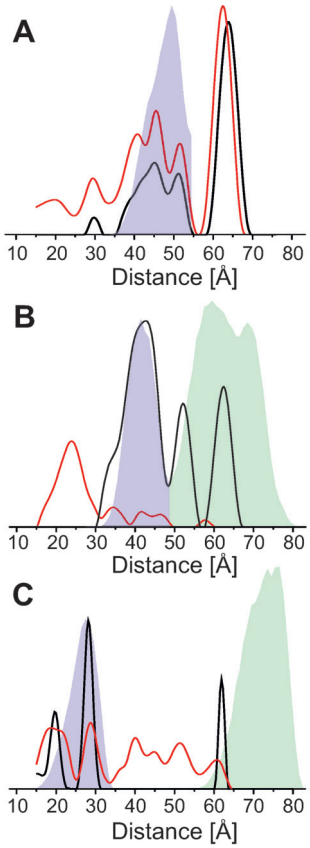

Figure 2. Distance distributions of holo- (black trace) and apoprotein (red trace) samples containing cysteine pairs at positions 302–353 (A), 195–267 (B), and 267–302 (C). Shaded areas are predictions based on the crystal structure of chicken SO (PDB ID: 1SOX) using the PyMOL script "MtsslWizard"; simulations using the MMM package can be found in Figure S8. Blue: intramonomer distances; green: intermonomer distances.

Table 1: Distance constraints for calculation of the apoprotein structure by the ENM-approach derived from DEER distance distributions.

Labeled positions	Weighted mean distance [Å]	Width of distribution [Å]
195–235	25.7	17.2
195–302	26.9	17.1
235–302	25.8	22.2
217–302	40.9	15.0
302–341	36.3	19.7
267–302	34.0	41.3
302–353	39.0	37.0
195–267	27.0	34.3
267–353	28.8	31.2

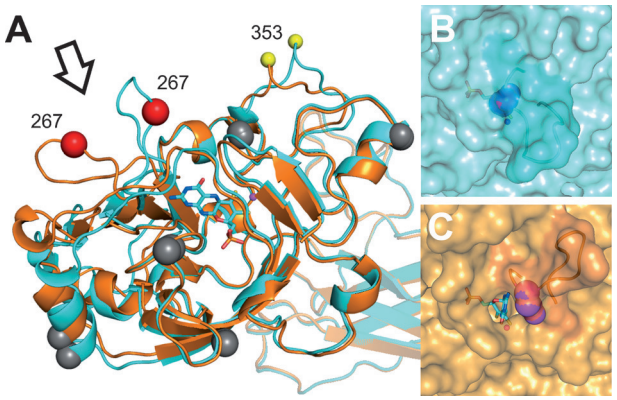

Figure 3. A) Structural model of the apo form (orange) of hSOMD as calculated by the ENM approach. Cyan: Holo form of cSO (PDB ID: 1SOX) used as reference structure. The dimerization domain is shown partially transparent. B, C) Section of the Connolly surface containing the loop 263–273 for the hSO structures shown in A where the viewing direction is indicated by an arrow. B) Holoprotein structure; the surface of the loop region and the loop backbone are highlighted. Side-chain atoms of residue D265 are shown as blue/magenta spheres; Moco is shown as a stick model. C) Structure of the apoprotein; for better visualization of access to the Moco binding pocket, the Moco has been drawn as a stick model in the apoprotein; the surface of the loop region and the loop backbone are highlighted. Side-chain atoms of residue D265 are shown as orange/magenta spheres.

the loop containing residue 267 undergoes Moco-dependent structural rearrangement. It should be noted that the distance distribution of pair 267–353 is broadened even for the holo form of the protein compared to expectations based on the crystal structure (Figure S7). This observation is in line with results from crystallography that reveal a loss of electron density for the loop containing residue 353 for a variant lacking the essential cysteine residue C207, which points towards increased mobility for this structural element (PDB ID: 3HBG).[20]

The structural constraints imposed by the measured distance distributions were used to describe the movement of the loop containing residue 267. DEER-derived data were used to calculate the structural transition by employing the "Elastic Network Model" (ENM) module of the Matlab toolbox "MMM2013.2".[21]

The distance distributions determined for the holoprotein fit well the expectation based on the cSO crystal structure (PDB ID: 1SOX). Hence, this structure was used as the reference point (without the heme domain) for the structural transition. The constraints (weighted mean value and width of the distribution, see Table 1) derived from the measurements of all cysteine pairs of the apo protein mentioned above were used and resulted in a calculated structure of the apo form as shown in Figure 3A (orange) in comparison to the crystal structure of cSO (cyan). The root-mean-square deviation (RMSD) of the optimized structure is found to be 1.6 Å, which is a value considered to indicate an acceptable fit.[21a]

The overlay of the two models reveals a large-scale movement of the loop containing residue 267 (red spheres). A smaller movement is also observed for the loop including residue 353 (yellow spheres), while no significant differences are observed for the other residues (grey spheres) investigated here. The movement of the loop containing residue 353 is most likely due to structural differences originating from the C207S exchange as discussed above.[20]

Analysis of the DEER experiments using the ENM approach on apoprotein samples demonstrate a flap-like movement of the short loop consisting of residues 263–273 in the absence of Moco, while the rest of the protein is virtually

unperturbed. This is the first direct experimental evidence for a structural change between holo-hSO and apo-hSO and confirms a proposal by Hille et al., who suggested the movement of a secondary structure element as part of the Moco incorporation mechanism for SO from *Arabidopsis thaliana*.[1b] It may be noted in passing that this highly localized structural rearrangement is different from other well-studied protein–cofactor interactions, which typically result in extensive and long-range effects upon binding (or removal) of the cofactor.[22] Comparing the Connolly surface[23] of the holo and the apo forms of the protein as shown in Figure 3B and C, respectively, shows that the flap-like movement in the apo form provides direct access to the Moco binding pocket from the outer surface, while this access is blocked by loop 263–273 in the holo form. The conformation of the loop in the holo form is stabilized by two hydrogen bonds from the D265 side chain to the N1 ring position and the 2-amino group of the Moco (Figure 3b).[11] It is important to note that this analysis is not meant to provide information on the loop conformation itself. These details depend on the specific input parameters of the simulation. However, all performed simulations show a movement of the loop such that the Moco binding pocket becomes accessible from the outer surface in the apoprotein (see the Supporting Information for a more detailed discussion). This finding provides a possible structural explanation for the in vitro reconstitution of Moco into hSO in the absence of additional proteins.[24] However, the incorporation process in vivo may involve additional proteins to optimize the maturation process of the enzyme in a manner similar to the dedicated chaperones identified for molybdoenzymes in prokaryotes.[25]

As discussed above, residue D265 plays an important role in Moco binding. It blocks the channel once the holoprotein is formed and keeps the Moco and loop in a defined conformation. Comparison with other proteins from the sulfite oxidase family reveals remarkable similarities in this Moco binding motif: Analogous loop structures with similar coordination to the Moco mentioned above are found, for example, in sulfite oxidase from *Arabidopsis thaliana* (residues 160–171, PDB ID: 1OGP) and sulfite dehydrogenase from *Starkeya novella* (residues 157–167, PDB ID: 2BPB) or *Escherichia coli* YedY (residues 43–52, PDB ID: 1XDQ; structural models and additional examples can be found in Figure S12). In light of the results found for hSO in this study, a similar mechanism of Moco incorporation involving the flap-like movement of the conserved loop structure for a range of vastly different organism can be expected.

In conclusion, we were able to show that structural differences between the apo and holo forms of hSO are restricted to a small loop region of the protein containing residues 263–273. A flap-like motion of the loop provides a structural explanation for the observed ability to insert Moco into apo-hSO in vitro. The conservation of this structural motif as well as the conserved interaction of analogous residues with the Moco throughout a range of mononuclear molybdoenzymes suggests that the structural changes observed for hSO and the proposed insertion mechanism apply to other homologouous proteins within this family as well.

Acknowledgements

We are grateful to the Center of Excellence 314 (UniCat) funded by the DFG for financial support. A.H. thanks the Studienstiftung des deutschen Volkes for a fellowship. We thank K. V. Rajagopalan (Duke University) for providing plasmids for the expression of hSO and hSOMD. We thank Ricarda Ebert for her help in the early stages of this project. We thank Gregor Hagelüken for adapting the PyMOL script "MtsslWizard" to the spin-labeled version of the non-natural amino acid *p*-acetylphenylalanine. The molecular biology part of this study was done in the molecular biophysics laboratory of the Department of Physics of FU Berlin.

Keywords: biocatalysis · cofactors · enzymes · EPR spectroscopy · protein structures

How to cite: *Angew. Chem. Int. Ed.* **2015**, *54*, 11865–11869
Angew. Chem. **2015**, *127*, 12033–12037

[1] a) G. Schwarz, R. R. Mendel, M. W. Ribbe, *Nature* **2009**, *460*, 839–847; b) R. Hille, J. Hall, P. Basu, *Chem. Rev.* **2014**, *114*, 3963–4038; c) G. Schwarz, R. R. Mendel, *Annu. Rev. Plant Biol.* **2006**, *57*, 623–647.
[2] S. H. Mudd, F. Irreverre, L. Laster, *Science* **1967**, *156*, 1599–1602.
[3] J. L. Johnson, W. R. Waud, K. V. Rajagopalan, M. Duran, F. A. Beemer, S. K. Wadman, *Proc. Natl. Acad. Sci. USA* **1980**, *77*, 3715–3719.
[4] V. E. Shih, I. F. Abroms, J. L. Johnson, M. Carney, R. Mandell, R. M. Robb, J. P. Cloherty, K. V. Rajagopalan, *N. Engl. J. Med.* **1977**, *297*, 1022–1028.
[5] a) J. Kuper, A. Llamas, H. J. Hecht, R. R. Mendel, G. Schwarz, *Nature* **2004**, *430*, 803–806; b) B. M. Hover, A. Loksztejn, A. A. Ribeiro, K. Yokoyama, *J. Am. Chem. Soc.* **2013**, *135*, 7019–7032.
[6] J. Teschner, N. Lachmann, J. Schulze, M. Geisler, K. Selbach, J. Santamaria-Araujo, J. Balk, R. R. Mendel, F. Bittner, *Plant Cell* **2010**, *22*, 468–480.
[7] a) M. Kaupp, *Angew. Chem. Int. Ed.* **2004**, *43*, 546–549; *Angew. Chem.* **2004**, *116*, 554–558; b) R. A. Rothery, B. Stein, M. Solomonson, M. L. Kirk, J. H. Weiner, *Proc. Natl. Acad. Sci. USA* **2012**, *109*, 14773–14778.
[8] J. M. Klein, G. Schwarz, *J. Cell Sci.* **2012**, *125*, 4876–4885.
[9] T. Kruse, C. Gehl, M. Geisler, M. Lehrke, P. Ringel, S. Hallier, R. Hansch, R. R. Mendel, *J. Biol. Chem.* **2010**, *285*, 6623–6635.
[10] C. Iobbi-Nivol, S. Leimkühler, *Biochim. Biophys. Acta Bioenerg.* **2013**, *1827*, 1086–1101.
[11] C. Kisker, H. Schindelin, A. Pacheco, W. A. Wehbi, R. M. Garrett, K. V. Rajagopalan, J. H. Enemark, D. C. Rees, *Cell* **1997**, *91*, 973–983.
[12] R. M. Garrett, D. B. Bellissimo, K. V. Rajagopalan, *Biochim. Biophys. Acta Gene Struct. Expression* **1995**, *1262*, 147–149.
[13] G. Jeschke, *Annu. Rev. Phys. Chem.* **2012**, *63*, 419–446.
[14] a) C. A. Temple, T. N. Graf, K. V. Rajagopalan, *Arch. Biochem. Biophys.* **2000**, *383*, 281–287; b) S. Reschke, D. Niks, H. Wilson, K. G. Sigfridsson, M. Haumann, K. V. Rajagopalan, R. Hille, S. Leimkühler, *Biochemistry* **2013**, *52*, 8295–8303; c) H. J. Cohen, S. Betcher-Lange, D. L. Kessler, K. V. Rajagopalan, *J. Biol. Chem.* **1972**, *247*, 7759–7766.
[15] a) R. M. Garrett, K. V. Rajagopalan, *J. Biol. Chem.* **1996**, *271*, 7387–7391; b) G. N. George, R. M. Garrett, R. C. Prince, K. V. Rajagopalan, *Inorg. Chem.* **2004**, *43*, 8456–8460.
[16] a) M. R. Fleissner, E. M. Brustad, T. Kalai, C. Altenbach, D. Cascio, F. B. Peters, K. Hideg, S. Peuker, P. G. Schultz, W. L. Hubbell, *Proc. Natl. Acad. Sci. USA* **2009**, *106*, 21637–21642;

b) A. Hahn, S. Reschke, S. Leimkühler, T. Risse, *J. Phys. Chem. B* **2014**, *118*, 7077 – 7084; c) C. C. Liu, P. G. Schultz, *Annu. Rev. Biochem.* **2010**, *79*, 413 – 444.
[17] G. Hagelueken, R. Ward, J. H. Naismith, O. Schiemann, *Appl. Magn. Reson.* **2012**, *42*, 377 – 391.
[18] G. Jeschke, V. Chechik, P. Ionita, A. Godt, H. Zimmermann, J. Banham, C. R. Timmel, D. Hilger, H. Jung, *Appl. Magn. Reson.* **2006**, *30*, 473 – 498.
[19] T. von Hagens, Y. Polyhach, M. Sajid, A. Godt, G. Jeschke, *Phys. Chem. Chem. Phys.* **2013**, *15*, 5854 – 5866.
[20] J. A. Qiu, H. L. Wilson, M. J. Pushie, C. Kisker, G. N. George, K. V. Rajagopalan, *Biochemistry* **2010**, *49*, 3989 – 4000.
[21] a) G. Jeschke, *Z. Phys. Chem.* **2012**, *226*, 1395 – 1414; b) G. Jeschke, *J. Chem. Theory Comput.* **2012**, *8*, 3854 – 3863; c) Y. Polyhach, E. Bordignon, G. Jeschke, *Phys. Chem. Chem. Phys.* **2011**, *13*, 2356 – 2366; d) Y. Polyhach, G. Jeschke, *Spectroscopy* **2010**, *24*, 651 – 659.
[22] a) M. Zhang, T. Tanaka, M. Ikura, *Nat. Struct. Biol.* **1995**, *2*, 758 – 767; b) H. M. Berman, L. F. Ten Eyck, D. S. Goodsell, N. M. Haste, A. Kornev, S. S. Taylor, *Proc. Natl. Acad. Sci. USA* **2005**, *102*, 45 – 50; c) A. C. Newton, *Chem. Rev.* **2001**, *101*, 2353 – 2364.
[23] M. Connolly, *J. Appl. Crystallogr.* **1983**, *16*, 548 – 558.
[24] S. Leimkühler, K. V. Rajagopalan, *J. Biol. Chem.* **2001**, *276*, 1837 – 1844.
[25] S. Leimkühler, W. Klipp, *J. Bacteriol.* **1999**, *181*, 2745 – 2751.

Received: May 26, 2015
Revised: June 29, 2015
Published online: August 18, 2015

